CrossMark

Determination of electronic ground state properties of a dinuclear iron(II) spin crossover complex

T. O. Bauer[1] · M. Schmitz[2] · M. Graf[2] · H. Kelm[2] ·
H.-J. Krüger[2] · V. Schünemann[1]

Abstract The dinuclear complex [(Fe(L-N$_4$Me$_2$))$_2$(BiBzIm)](ClO$_4$)$_2 \cdot$ 2EtCN **(1)** has been investigated by Mössbauer spectroscopy carried out in the temperature range from 5 to 150 K with externally applied magnetic fields of up to B = 5 T. By means of a consistent simulation of all experimental data sets within the Spin Hamiltonian formalism, the zero-field splitting D and the rhombicity parameter E/D of the ferrous high-spin (HS) site in this complex was determined to be $D = -15.0 \pm 1.0$ cm^{-1} and $E/D = 0.33$ respectively. The sign of the quadrupole splitting of the HS site is positive which indicates that this iron site of the dinuclear complex **1** has an electronic ground state with the d$_{xy}$ orbital being twofold occupied.

Keywords Mössbauer spectroscopy · Spin crossover · Molecular magnetism · Zero-field splitting

1 Introduction

Iron (II) spin crossover (SCO) systems [1, 2] provide interesting materials for future sensor and memory devices [3]. They can be switched reversibly from the low-spin (LS) state (S = 0) to the high-spin (HS) state (S = 2) by variation of temperature, pressure or by irradiation with light [1]. The dinuclear compound [(Fe(L-N$_4$Me$_2$))$_2$(BiBzIm)](ClO$_4$)$_2 \cdot$
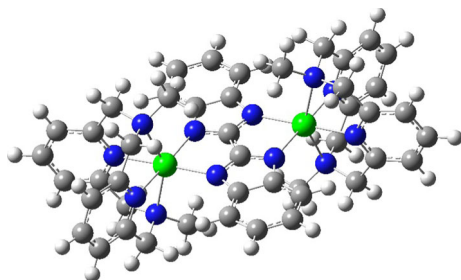
✉ T. O. Bauer
    thbauer@rhrk.uni-kl.de

1   Department of Physics, University of Kaiserslautern, Erwin-Schrödinger-Str. 46, 67663
    Kaiserslautern, Germany

2   Department of Chemistry, University of Kaiserslautern, Erwin-Schrödinger-Str. 54, 67663
    Kaiserslautern, Germany

🙼 Springer

Fig. 1 Perspective view of **1**, after [4]. The two iron ions of the complex are shown in *green*

2EtCN (**1**) exhibits an abrupt spin crossover at T = 175 K [4]. Because of the intramolecular cooperativity communicated via the bridging-ligand this complex has not a LS-LS but a LS-HS ground state [4]. Here, we report on the characterization of this complex by means of temperature- and field- dependent Mössbauer spectroscopy. The aim of this study is to characterize the electronic ground state of the HS iron site in the dinuclear iron complex and to determine its zero field splitting D and its rhombicity parameter E/D.

2 Materials and methods

A perspective view of the molecular structure of **1** is shown in Fig. 1. Structural details were discussed in ref. [4]. Mössbauer spectra were recorded with a 1.85 GBq ^{57}Co(Rh) source on powder samples embedded in polyethylene foil Leukoflex$^{®}$ in transmission geometry and constant acceleration mode. The measurements obtained at high magnetic fields were performed with a closed cycle cryostat equipped with a superconducting magnet as described earlier [5]. Magnetically split spectra were simulated on the basis of the Hamiltonian approximation using Vinda Add On for Excel 2003 [6].

In order to calculate the spin expectation values $< \vec{S} >$ the following Hamiltonian was used [7–9]:

$$\widehat{H}_S = D\left[\widehat{S}_z^2 - S(S+1)/3 + E/D\left(\widehat{S}_x^2 - \widehat{S}_y^2\right)\right] + \mu_B\vec{S}\cdot\overleftrightarrow{g}\cdot\vec{B} \quad (1)$$

where S is the spin quantum number of the electronic ground state, D the zero field splitting, E/D the rhombicity parameter and μ_B the bohr magneton. High-field Mössbauer spectra were simulated using (1) together with the nuclear Hamiltonian [7–9]:

$$\hat{H}_N = \frac{eQV_{zz}}{4I(2I-1)}\left[3\hat{I}_z^2 - I(I+1) + \eta\left(\hat{I}_x^2 - \hat{I}_y^2\right)\right] - g_N\mu_N\vec{I}\cdot\vec{B} + <\vec{S}>\cdot\overleftrightarrow{A}\cdot\vec{I} \quad (2)$$

Here I denotes the spin quantum number of the nuclear states, Q the nuclear quadrupole moment, V_{zz} the z-component of the electric-field gradient (efg) tensor, and $\eta = (V_{xx} - V_{yy})/V_{zz}$ the asymmetry parameter of the efg. $\overleftrightarrow{A}$ represents the hyperfine coupling tensor which couples $< \vec{S} >$ to the nuclear spin $\vec{I}$ and g_N is the nuclear g-factor.

3 Results and discussion

The Mössbauer spectrum of **1** obtained at 5 K with a small applied field of 20 mT exhibits two quadrupole doublets with an intensity ratio of 1:1 (Fig. 2). Component 1 has
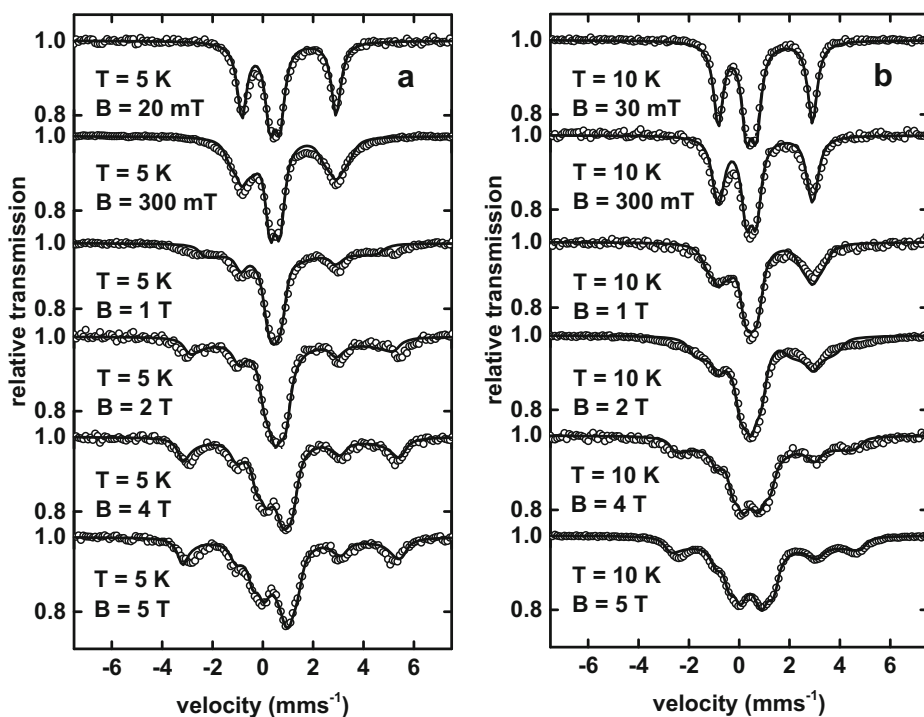
Fig. 2 Field dependent Mössbauer spectra of **1** taken at T = 5 K (**a**) and at T = 10 K (**b**) with indicated external fields varied from 20 mT to 5 T applied perpendicular to the γ-beam. The *solid lines* are the result of a spin-Hamiltonian analysis including simultaneous fitting of all displayed data sets. The resulting parameters are given in Table 1. The simulations corresponding to the data measured at 5 K in (**a**) were obtained in the slow-relaxation limit and those corresponding to the data measured at 10 K in the fast relaxation limit

$\delta_1 = 0.48$ mms^{-1} and $\Delta E_{Q1} = 0.39$ mms^{-1}. The low value of ΔE_{Q1} indicates that component 1 arises from the diamagnetic ferrous LS site of the complex. Component 2 has $\delta_2 = 1.04$ mms^{-1} and $\Delta E_{Q2} = 3.74$ mms^{-1}, the isomer shift of which is typical for a ferrous HS site. An increase of the external applied field to 300 mT and further up to 5 T induces a complex, magnetically split pattern. In order to reproduce the field dependent Mössbauer spectra spin Hamiltonian simulations have been performed. With the parameter set displayed in Table 1 a consistent reproduction of all the experimental data sets was achieved (see solid lines in Fig. 2).

Component 1 is consistent with a diamagnetic ferrous LS site. This site shows an asymmetry parameter of $\eta_1 = 1$. Therefore the sign of the electric field gradient is not defined ($\Delta E_{Q1} = (\pm) 0.39$ mms^{-1}).

Component 2 represents the ferrous HS site of the complex. The electronic spin expectation value $<\vec{S}>$ of the HS site is coupled to the nuclear spin $\vec{I}$ via an anisotropic hyperfine coupling tensor ($A/\mu_N g_N = (-67.0, \leq +10.0, -8.6)$ T). The electric field gradient of site 2 is axial ($\eta_2 = 0$). The simulations yield a large and negative zero-field splitting of the ferrous HS site 2 ($D = -15.0$ cm^{-1}) with a maximum value of the rhombicity parameter ($E/D = 0.33$). It should be noted that only an estimated upper limit of A_{yy} could be given. This originates from the fact that for a $S = 2$ spin system in the case of a negative D and $E/D \sim 0.33$, the largest component of $<\vec{S}>$ is orientated along the z-direction and nearly

Table 1 Parameters obtained by the spin Hamilton simulations (solid lines) shown in Figs. 2 and 3

Component	S	δ/mms^{-1}	ΔE_Q /mms^{-1}	D/cm^{-1}	E/D	$A_{xx,yy,zz}$/$\mu_N g_N$/T
1	0	0.48($\pm$0.03)	$\pm$0.39($\pm$0.03)	–	–	–
2	2	1.04($\pm$0.03)	+3.74($\pm$0.03)	$-15(\pm1)$	0.33($\pm$)0.02	$-67(\pm2)$, $< +10$, $-8.6(\pm0.5)$

The exp. area of the two components was set 1:1, the line width was $\Gamma = 0.45$ mms^{-1} and the asymmetry parameter was $\eta_1 = 1$ for the LS site 1 and $\eta_2 = 0$ for the HS site 2. In addition $\beta = 98°$ has been used for component 2. This is the Euler angle which rotates the main axis system of the A tensor relative to that of the zero-field splitting tensor. The Zeeman term was assumed to be isotropic, with g = 2
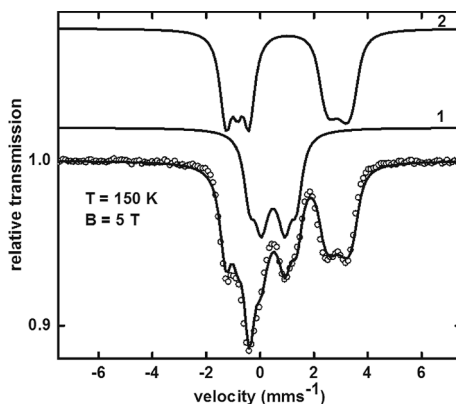
Fig. 3 Mössbauer spectrum of **1** taken at T = 150 K with an external field of B = 5 T applied perpendicular to the γ-beam. The *solid line* is a result of a spin-Hamiltonian simulation, representing the diamagnetic LS site 1 and the paramagnetic HS site 2. The relative area of component 1 is 43 % instead of 50 % which may be caused by either the onset of SCO and/or slightly different Lamb-Mössbauer factors of HS and LS iron(II) ions at T = 150 K. The simulation has been performed with the parameters shown in Table 1 using the fast relaxation limit

zero in y-direction. The magnitude and sign of the zero-field splitting, the combination of negative zero-field splitting and maximal rhombicity is similar to those found for other ferrous high spin complexes [10–13]. It is however interesting to note, that a related dinuclear complex ([{Fe(L-N$_4$Me$_2$) }$_2$(BzImCOO)](ClO$_4$)$_2$ ∗ 0.5(CH$_3$)$_2$CO (**2**)) [4] has an HS iron site which has a positive D and a significant lower value of the rhombicity (D = 7.2 cm^{-1} and E/D = 0.1) [13]. In comparison to the complex **1** discussed in this study the former complex has a different bridging ligand. This obviously has a significant influence on the degree of orbital momentum quenching in the molecule which might cause the observed differences in the values of the fine structure parameters D and E/D.

Additionally the positive sign of the quadrupole splitting ($\Delta E_{Q2} = +3.74$ mms^{-1}) as well as the axial character of the electric field gradient ($\eta_2 = 0$) of the HS iron site of complex **1** have been verified by the analysis of a Mössbauer spectrum which was taken at T = 150 K in an external field of 5 T. At such temperature the S = 2 spin multiplets are almost equally populated and the internal fields average to zero resulting in a quasi diamagnetic Mössbauer spectrum (see Fig. 3) [7–9, 14].

The electronic ground state of **1** can be determined using the Townes-Dailey approximation [15, 16]. The assumption that the electronic contribution to the electric field gradient

dominates a ferrous HS iron site with $\Delta E_Q > 0$ leads to the conclusion that complex **1** has an electronic ground state with a twofold occupied d_{xy} orbital. Also the HS site of complex **2** mentioned above has a d_{xy} electronic ground state [13]. Thus the different bridging ligands of **1** and **2** do not influence the electronic ground state but lead to differences in D and E/D. The origin of this effect is not yet clear and quantum chemical calculations may help to resolve this issue.

References

1. Gütlich, P., Goodwin, H.A.: Top. Curr. Chem. **233**, 1–48 (2004)
2. Gütlich, P., Gaspar, A.B., Garcia, Y.: Beilstein J. Org. Chem. **9**, 342–391 (2013)
3. Salmon, L., Molnar, G., Zitouni, D., Quintero, C., Bergaud, C., Micheau, J.-C., Bousseksou, A.: J. Mater. Chem. **20**, 5499–5503 (2010)
4. Krüger, H.-J.: Coord. Chem. Rev. **253**, 2450–2459 (2009)
5. Janoschka, A., Svenconis, G., Schünemann, V.: J. Phys. **217**, 1–4 (2010)
6. Gunnlaugsson, H.P.: Vinda Excel Add-On. http://users-phys.au.dk/hpg/vinda.htm Accesed: 13.08.15
7. Huynh, B.H., Kent, T.A.: In: Eichhorn, G.L., Marzilli, L.G. (eds.) Advances in Inorganic Biochemistry. Elsevier, New York, Amsterdam, Oxford (1984)
8. Debrunner, P.G.: In: Lever, A.B.P., Gray, H.B. (eds.) Iron Porphyrins, part III, VCH, Weinheim, pp. 139–234 (1989)
9. Trautwein, A.X., Bill, E., Bominaar, E.L., Winkler, H.: Struct. Bond. **78**, 1–95 (1991)
10. Stoian, S.A., Smith, J.M., Holland, P.L., Münck, E., Bominaar, E.L.: Inorg. Chem. **47**, 8687–8695 (2008)
11. Zimmermann, R., Huynh, B.H., Münck, E., Lipscomb, J.D.: J. Chem. Phys. **12**, 69 (1978)
12. Bominaar, E.L., Ding, X.-Q., Gismelseed, A., Bill, E., Winkler, H., Trautwein, A.X., Nasri, H., Fischer, J., Weiss, R.: Inorg. Chem. **31**, 1845–1854 (1992)
13. Bauer, T.O., Schmitz, M., Graf, M., Kelm, H., Krüger, H.-J., Schünemann, V.: Hyperfine Interact. **226**, 359–363 (2014)
14. Collins, R.L., Travis, J.C.: In: Gruvermann, I.J. (ed.) Mössbauer Effect Methodology, vol. III. Plenum Press, New York (1967)
15. Townes, C.H., Dailey, P.P.J.: Chem. Phys. **17**, 782–796 (1949)
16. Keutel, H., Käpplinger, I., Jäger, E.-G., Grodzicki, M., Schünemann, V., Trautwein, A.X.: Inorg. Chem. **38**, 2320–2327 (1999)